Available online at www.sciencedirect.com
ScienceDirect
Combustion and Flame 151 (2007) 37–45
Combustion and Flame
www.elsevier.com/locate/combustflame

Application of molecular beam mass spectrometry in studying the structure of a diffusive counterflow flame of CH_4/N_2 and O_2/N_2 doped with trimethylphosphate

D.A. Knyazkov, A.G. Shmakov, O.P. Korobeinichev *

Institute of Chemical Kinetics & Combustion, Novosibirsk 630090, Russia

Received 1 June 2006; received in revised form 12 June 2007; accepted 25 June 2007

Available online 7 August 2007

Abstract

The applicability of molecular beam mass spectrometry (MBMS) in studying the structure of counterflow flames has been tested by investigating a counterflow flame of CH_4/N_2 and O_2/N_2. The thermal structure of the flame was examined using a microthermocouple; the concentration profiles of such stable species as CH_4, O_2, and CO_2 were measured by sampling with a microprobe and MBMS at various positions. The microprobe did not disturb the flame. However, the sonic probe, when inserted into the flame transverse to the burner axis to measure the centerline concentration profiles, produced a significant disturbance of the flame. But no such disturbance was observed when the tip of the sonic probe was located at the periphery of the burner. Good agreement was obtained between the concentration profiles of stable species, as measured using a microprobe and a sonic probe at the periphery of the burner. To verify the applicability of MBMS for detecting radicals and other labile species in a counterflow flame, the concentration profiles of H, OH, and the main phosphorus-bearing species in the counterflow flame doped with trimethylphosphate (TMP) were measured by MBMS at the periphery of the burner and compared with results of modeling using the OPPDIF code and a mechanism for the combustion of TMP, tested previously in premixed flames of methane and oxygen with TMP as an additive. Good agreement was obtained between the measured and simulated concentration profiles for the reagents, as well as for the final and intermediate products with relatively high molecular weights (PO, PO_2, HOPO, $HOPO_2$). The measured concentration profiles of species with low molecular weights (H_2O, CO_2, OH, H) were found to be broader than the calculated ones—in fact, the lower the molecular weight, the wider was the profile. This is probably due to a real flame not being one-dimensional.

Keywords: Molecular beam mass spectrometry; Counterflow flames; Flame structure; Inhibition; Phosphorus-containing compounds

1. Introduction

Molecular beam mass spectrometry (MBMS) is one of the most effective techniques for studying the chemical structure of a flame. It allows one to iden-

* Corresponding author. Fax: +7 383 3307350.
E-mail address: korobein@kinetics.nsc.ru (O.P. Korobeinichev).

0010-2180/$ – see front matter
doi:10.1016/j.combustflame.2007.06.011

tify both stable and labile species, including atoms and free radicals, as well as to measure their concentrations and their spatial distributions. A comparison of experimental results with modeling of the structure of a flame provides information on the mechanisms and kinetics of the major chemical reactions occurring. Although MBMS has been widely used to explore the chemical structure of flames stabilized on a flat burner, there have been no MBMS studies of the structure of counterflow diffusion flames, which have recently become a subject of increased interest. In previous studies e.g., [1–5], the structure of counterflow flames has been studied by sampling with a quartz microprobe with a subsequent chromatographic analysis of the sample. A major advantage of sampling with a microprobe is the negligible thermal and gas-dynamic perturbations of the flame induced by a microprobe. Quenching a chemical reaction in the sample and thus the measurements of concentration profiles are known to depend significantly on such parameters of the probe as its internal angle, the diameter of the orifice, and the nature of its internal surface, because heterogeneous reactions do take place on the hot inner walls of the microprobe. Consequently, with a microprobe, labile species (atoms, radicals), as well as many stable species, can decompose or react on the inner walls of the microprobe as well as in the gas phase. In the above papers as well as in many other works, only the size of the orifice (∼0.06–0.5 mm) and the diameter (∼0.1–1 mm) of the outer tip were specified. However, the value of the internal angle does not allow one to estimate the quality of the measurements. Of course, the internal angle of the cone characterizes the sample's freezing. Gas-phase chemical reactions are known [6] to occur in probes with too wide an internal angle. Height et al. [7] attached an alumina capillary to an alumina tube (O.D. 1.6 mm) as a probe for studying the structure of counterflow natural gas/air flames. Choking in the probe should be experimentally verified by measuring flow rates of postflame gases through the microprobe, while varying the back pressure in the sampling system, similarly to [8,9]. However, in most works, this testing was not carried out. We conclude that using capillaries or microprobes with small cone angles for gas sampling can cause errors in measurements of concentrations in a flame.

A diffusive counterflow flame of CH_4/N_2 and O_2/N_2 doped with trimethylphosphate (TMP) is very appropriate for verifying the applicability of MBMS, which has been extensively used to study the structure of premixed flames doped with organophosphorus compounds (OPCs) [10–24]. It has been shown that the phosphorus oxides catalyze the recombination of the radicals H, O, and OH [15–17] and so play a key role in flame inhibition by OPCs. Several detailed reaction mechanisms for OPCs, including TMP, have been developed previously [10,19,25–28], but there are still significant gaps and uncertainties in the inhibition mechanism. In addition, there are discrepancies between experiments and simulations. To improve existing kinetic models, one needs a wide range of measurements of the structure and burning velocity of premixed and diffusion flames. One gap is in experiments on the structure of counterflow flames with OPCs as additives. Laser-induced fluorescence (LIF) has been used to measure concentration profiles for OH radicals in counterflow flames doped with OPCs [10,12,13,29,30]. However, it is especially necessary to also have experimental profiles of both stable and labile species, such as the hydrogen atom, PO and PO_2 radicals, and other P-bearing species, such as HOPO, $HOPO_2$, and $PO(OH)_3$. The latter cannot be detected by microprobe sampling techniques or LIF. MBMS studies of the structure of counterflow flames doped with OPCs have not been reported until now. This study is of a counterflow diffusion flame of CH_4/N_2 and O_2/N_2 without an additive and with TMP added to the oxidizer flow. The goal of this work was to verify the applicability of MBMS in determining the structure of counterflow flames. In addition, this MBMS study aims to validate a previously developed mechanism of flame inhibition by OPCs by comparing measurements with the results of simulations of flame structure.

2. Experimental details

A counterflow diffusion flame of CH_4/N_2 (0.2/0.8) and O_2/N_2 (0.4/0.6) was stabilized on an opposed-jet burner at atmospheric pressure (755 ± 5 Torr). Fig. 1 shows the burner. The reactants passed through nozzles, which were straight quartz tubes; flowing nitrogen was used as a sheath. The volumetric flow rates for the streams of fuel and oxidizer under ambient conditions were both 20 ml/s and were set with an

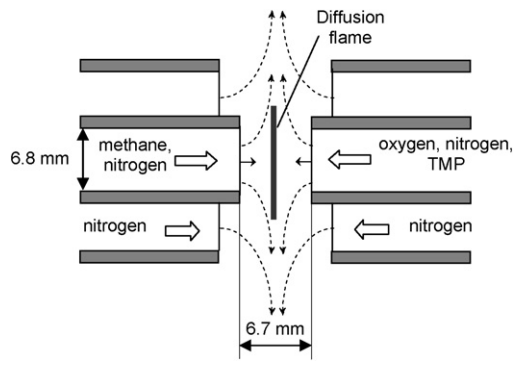

Fig. 1. Counterflow burner.

accuracy of ∼1%, being controlled by mass flow controllers (MKS Instruments) operated by a PC.

The flame had a global strain rate of 358 s^{-1}, as calculated using the equation [31]

$$a = \frac{2V_{ox}}{L}\left(1 + \frac{V_f}{V_{ox}}\left(\frac{\rho_f}{\rho_{ox}}\right)^{1/2}\right), \quad (1)$$

where L is the separation distance between the nozzles, V is the mean axial velocity at the nozzle exit, and ρ is the gas density. The subscripts ox and f refer to the oxidizer and fuel, respectively.

TMP was added into the oxidizer flow using a nebulizer and a syringe pump. The nebulizer has been described earlier [32]. The oxidizer stream was maintained at 90 °C to ensure evaporation of the TMP aerosol and to prevent TMP from condensing onto the walls of the tubes. The distance between the nebulizer and the oxidizer nozzle was ∼22 cm. Estimates [18] show that the evaporation time of drops in the TMP aerosol is much less than the residence time of the drops in the oxidizer flow. The temperature of the fuel stream was 22–24 °C.

Spatial distributions of the concentrations of various species in the flame were obtained using microprobe and molecular beam sampling systems, coupled with a quadrupole mass spectrometer MS-7302 with soft ionization by electron impact. The results obtained by microprobe sampling are compared below with measurements using MBMS to verify the use of MBMS for the determining the structure of such a counterflow flame. The quartz microprobe was 100 mm long and constructed of 6.0-mm O.D., 3.8-mm I.D. quartz tubing, tapering to an orifice with a diameter of 0.04 mm; the wall thickness near the orifice was 0.08 mm and the opening angle near the orifice was 20°. The microprobe was connected to the inlet system of the mass spectrometer. The molecular beam mass spectrometric setup has also been detailed previously [33]. The opening angle of the "sonic" probe was 40°, the orifice diameter 0.08 mm, the wall thickness near the orifice 0.08 mm, and the height of the cone 22 mm. Ionization energies (IE) used for measurements of mass peak intensities and ionization potentials (IP) of the species are presented in Table 1. The reasons for preferring the IE values used have been given [23]. During the measurements, the opposed-jet burner axis was positioned horizontally, since the MBMS setup [33] does not allow the burner axis to be located vertically. The burner position was found not to affect the measurements of flame structure. This was justified by measurements of temperature profiles using a microthermocouple, which showed that temperature profiles do not depend on whether the burner's axis was vertical or horizontal.

Table 1
Ionization energies used for measurements of mass peak intensities and ionization potentials of the species

Compound	m/e	IP (eV)	IE (eV)
H	1	13.6[a]	16.2
CH_4	15	12.98[a]	18
OH	17	12.9[a]	16.2
H_2O	18	12.6[a]	16.2
O_2	32	12.07[a]	18
CO_2	44	13.79[a]	17.5
PO	47	8.2[a], 8.3[b]	12.8
PO_2	63	10.6[b]	12.8
HOPO	64	10.3[b]	12.8
$HOPO_2$	80	12.4[b]	14.5
TMP	140	9.76[a]	21

[a] Reference data [34].
[b] Data obtained in [23].

Temperature profiles along the axis of the burner and at a specified distance from the axis were obtained using a Pt–PtRh(10%) Π-shaped thermocouple [33] welded from wire 0.02 mm in diameter. To prevent catalytic processes on the thermocouple, it was coated with a thin layer of SiO_2. The total diameter of the thermocouple with the SiO_2 layer was 0.05 mm. The total length of the thermocouple's shoulders was 1 cm (i.e., greater than the outer diameter of the burner nozzles) to minimize any perturbations of the flame by the thermocouple. Radiation corrections for the SiO_2 coating were made using Kaskan's formula [35]. The errors in temperature measurements were ∼ ±40 K at the 95% confidence limit.

The concentrations of CH_4, O_2, CO_2, and TMP were determined using the relation

$$C = IC_0/I_0, \quad (2)$$

where C is concentration, I the intensity of a peak in the mass spectrum of a sample, and C_0 and I_0 are the values for a mixture of known composition. The errors in determining the concentrations of CH_4, O_2, and CO_2 were ∼ ±8%. Peak intensity profiles for H and OH in the doped flame were measured immediately after making measurements in the undoped flame. The errors in measuring the peak intensities for H and OH were ±24 and ±15%, respectively.

The simulations showed that at the point of maximum flame temperature, concentrations of P-compounds were close to those of thermodynamic equilibrium, within an accuracy of 20% (PO, PO_2), 30% (HOPO), or 10% ($HOPO_2$). Based on this, the calibration coefficients for P-bearing species were determined by comparing the equilibrium concentrations and mass peak intensities at the point with the maximum flame temperature. The resulting calibration coefficients were close to those obtained previously [21]. The error in measuring the intensities of

a peak corresponding to a P-species was $\sim \pm 10\%$ of the maximum peak intensities.

3. Modeling

Modeling of a counterflow flame was done using OPPDIF Code [36] from the Chemkin II Suite [37]. The calculations were performed for both potential and plug flow boundary conditions. These cases of boundary conditions are idealizations. The measurements indicate that the actual velocity field lies somewhere between the two approximations [38]. The calculations performed showed that the concentration profiles depend on the flow's boundary conditions only slightly. Therefore, in the present paper, we give only the numerical results for plug flow boundary conditions. In the calculations, we used the GRI 3.0 mechanism [39], thermochemical data for phosphorus species [41], and a detailed chemical kinetic mechanism for TMP [28], as validated on measurements of the burning velocity and structure of flat premixed methane flames doped with TMP [40].

4. Results and discussion

MBMS provides information about the spatial distribution of atoms, radicals, and other unstable species in a flame and thus offers an advantage over mass spectrometry with a microprobe. However, the perturbations of a flame by the microprobe are smaller than those by a "sonic" probe. Our visual observations showed that the "sonic" probe, when inserted into a flame at a right angle to the axis of the burner (for sampling parallel to this axis), produced a significant disturbance of the flame; i.e., the luminous disc of the flame was observed to be distorted considerably. However, similar insertion of the microprobe into the flame did not cause any such perturbation. Even so, no distortion of the flame's luminous disc was observed visually when the tip of the "sonic" probe was located at a distance $r = 3.3$ mm, i.e., at the periphery of the flame. This distance coincides with the inner radius of the burner's nozzles. In the OPPDIF code, all dependent variables were assumed to be functions only of the axial coordinate, so that concentrations did not depend on this radial coordinate. We checked this assumption experimentally by measuring the axial profiles of both temperature and concentration in a counterflow flame without additives and at various distances from the axis using the microprobe and microthermocouple. In addition, we calculated the profiles of temperature and concentrations along the burner's axis and compared the results with the measurements. Thus, Fig. 2 shows the calculated and measured temperature distributions in the flame along the burner axis at various radial distances from the axis in the range from $r = 0$ to 5 mm. The temperature profiles measured at distances from the burner axis of $r = 0$ to $r = d/2 = 3.3$ mm (d is the inner diameter of the burner nozzles) agree with each other and with the calculated profile within experimental error. However, the width of the experimental profiles for $r > d/2$ is greater than that for $r < d/2$. Thus, the results in Fig. 2 show that the thermal structure of this counterflow flame is one-dimensional at distances from the burner axis not exceeding the inner diameter of the burner nozzles.

Microprobe sampling was used to measure the concentration profiles of the stable species CH_4, O_2, and CO_2 along the axis at various r. Fig. 3 shows the results of microprobe sampling along the axis, i.e., at $r = 0$ (black symbols), and on the flame's periphery at $r = 3.3$ mm (gray symbols). Fig. 3 reveals

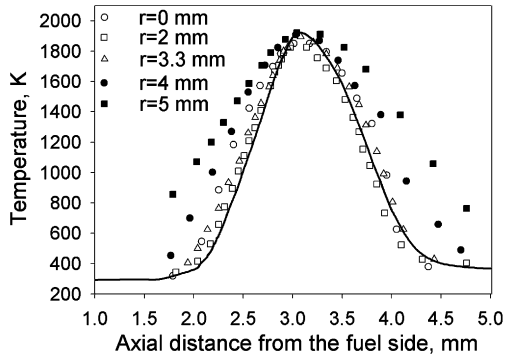

Fig. 2. Temperature distribution in undoped flame along the axis of the burner and at various distances r from the axis ($r = 0$ to 5 mm). Symbols show measurements; curves are computed results.

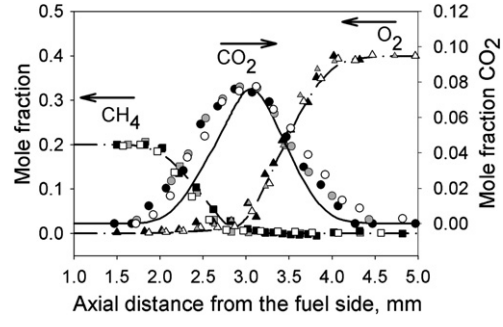

Fig. 3. Concentration profiles of some stable species in the flame. White symbols are measurements obtained with a "sonic" probe at the flame's periphery ($r = 3.3$ mm) using MBMS. Black and gray symbols are measurements obtained by microprobe sampling on the axis and at the flame's periphery, respectively. Curves are computed results.

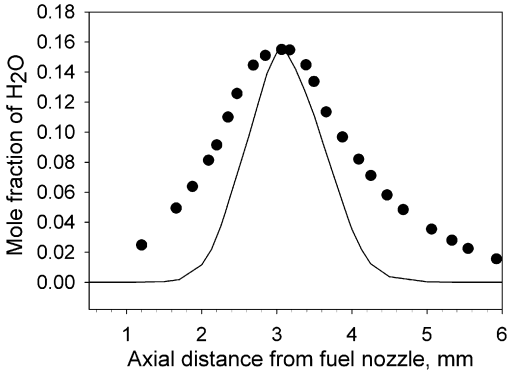

Fig. 4. Concentration profile of H_2O in undoped counterflow flame. MBMS measurements (symbols) were performed at the flame's periphery ($r = 3.3$ mm). The curve is the computed result.

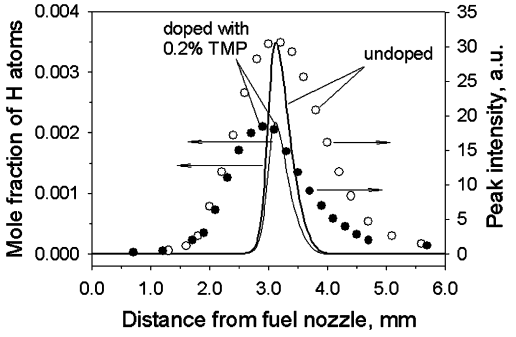

Fig. 5. Spatial distribution of [H] in the counterflow flame doped with 0.2% TMP and without additive. Experimental measurements (symbols) were obtained with MBMS at the flame's periphery ($r = 3.3$ mm). The curves are computed results.

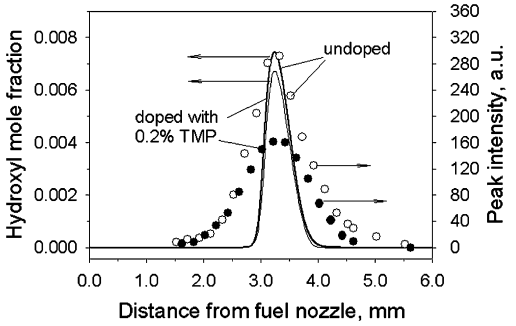

Fig. 6. Spatial distribution of [OH] in the counterflow flame doped with 0.2% TMP and also without an additive. MBMS measurements (symbols) were performed at the flame's periphery ($r = 3.3$ mm). The curves are computed results.

good agreement (within experimental error) between measurements at $r = 0$ and 3.3 mm and simulated concentration profiles of O_2 and CH_4. However, the measured concentration profile for CO_2 is broader than the calculated one. Since the "sonic" probe positioned at the periphery of the burner does not disturb the flame, it was used there for measuring the concentration profiles of stable species. These measurements are plotted in Fig. 3 (open symbols), together with the profiles obtained from microprobe sampling and modeling (curves). One can see that the experimental results obtained by the microprobe and "sonic" probe are in fairly good agreement with each other. This indicates that any perturbations of a flame by the "sonic" probe when sampling at the periphery of the flame (at $r = d/2$) do not exceed the perturbations by the microprobe. The measurements on the burner's periphery using MBMS, as well as the calculated concentrations profiles for H_2O, are shown in Fig. 4. The experimental profile is seen to be wider than the calculated one, as was observed for the profile of CO_2.

Figs. 5 and 6 show peak intensity profiles (in arbitrary units) obtained using MBMS for H atoms and hydroxyl radicals in the flame doped with 0.2% TMP and without additive (symbols). Modeling results (curves) are also presented in Figs. 5 and 6. The measurements and results of modeling indicate that the addition of 0.2% TMP reduces the peak concentrations of H and OH and the widths of the profiles. This agrees with LIF measurements [29,30], which noted that the addition of inhibitors (TMP or dimethylmethylphosphonate) to diffusion counterflow flames of methane and air reduced the maximum concentration of OH, as well as the width of its profile. The addition of TMP to lean and rich premixed flames of $CH_4/O_2/Ar$ stabilized on a flat burner also decreases [40] the concentrations of H and OH in the reaction zone, with the reduction of [H] being more severe than that of [OH]. However, no experimental information can be found in the literature on concentration profiles for [H] in diffusion counterflow flames. The reduction in maximum values of [H] and [OH] on adding TMP amounted to ∼38 and 45%, respectively. This is consistent with modeling of [H], but the calculated reduction of [OH] from its maximum is only 10%, i.e., considerably lower than determined experimentally. From Figs. 5 and 6, it is evident that the widths of the experimental profiles of [H] and [OH] at half maximum (FWHM) are greater than those predicted by ∼3.8 and 2.5 times, respectively. However, good agreement has been observed [29,30] between calculated [OH] profiles and those measured along the axis using the noninvasive LIF technique.

As shown before [29,30,42], the reduction in the total integrated [OH] is a very useful parameter for estimating the effectiveness of flame inhibitors, because it provides information on changes in both the peak concentration of OH and the width of its profile. Similarly, the effectiveness of an inhibitor can be

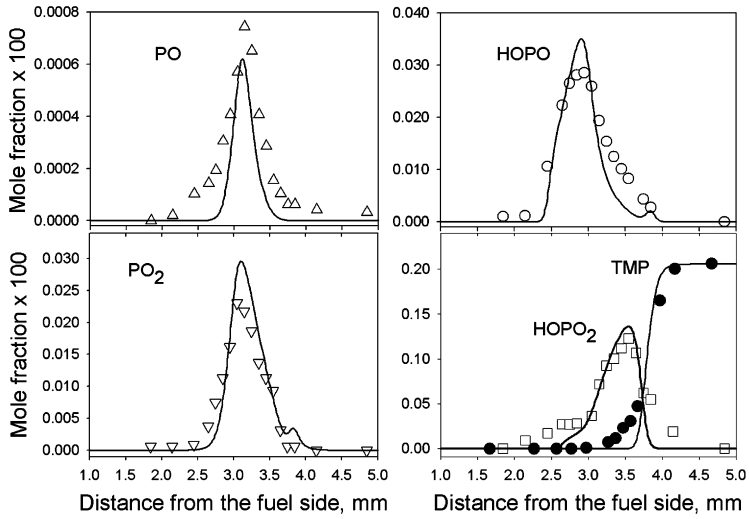

Fig. 7. Spatial distribution of major P-bearing species in the flame doped with 0.2% TMP. Symbols show experimental measurements; the curves are computed results.

estimated in terms of the reduction in the total integrated concentration of free H atoms. The reduction in the total integrated [H] on adding 0.2% TMP was measured to be 42%, but was 41% from the simulated profiles. This is good agreement, in spite of the considerable discrepancy between the FWHM of the measured and calculated profiles of [H]. A reduction of total integrated [H] by the presence of the dopant was justified by calculations modeling various loadings of the dopant. This substantiates the possibility of using this parameter for estimating the effectiveness of an inhibitor.

The broadening of the profiles of [H], [OH], [CO_2], and [H_2O] discovered above may be caused by two factors: the quasi-one-dimensional nature of the flame and perturbations of the flame induced by the probe. Neither of these factors was studied experimentally in this work. However, the results of a two-dimensional simulation of a counterflow flame of H_2/N_2 and O_2/N_2 [43] provided important evidence for the first factor. These results were compared with those obtained using the OPPDIF Code. The flame studied by Frouzakis et al. [43] was shown to be one-dimensional near the axis of the burner, but this broke down on moving away from the axis, especially for species with a high diffusivity (H, H_2, OH). These results [43] demonstrated that the profiles of [OH] and the temperature were wider near the edge of the burner tube than on the axis of symmetry. In fact, there was a more pronounced radial dependence of [OH] and temperature for $r > d/2$. Of course, it is impossible to apply these findings quantitatively to this study, because the results were obtained for counterflow flames with different compositions and under different conditions. However, comparing the modeling results [43] qualitatively with the above measurements, one can arrive at the following relation: the lower the molecular weight of the species (i.e., the greater the diffusion coefficient), the more dramatic is the widening of a concentration profile. In support of this claim, the diffusion coefficients for H, OH, H_2O, and CO_2 were determined at the maximum flame temperature (∼1960 K) using the CHEMKIN Code to be 33.4, 8.2, 7.3, and 4.2 cm^2/s, respectively. Another substantiation of the above claim is the satisfactory agreement between measured (using MBMS) and simulated concentration profiles of TMP, PO, PO_2, HOPO, and $HOPO_2$ in the counterflow flame doped with 0.2% TMP. These are presented in Fig. 7. The diffusion coefficients for these species differ from each other only slightly. At the maximum flame temperature, they range from 2.6 to 3.5 cm^2/s, i.e., less than for CO_2.

A probe is known [44] to generate thermal and gas-dynamic perturbations of a flame, especially when MBMS is used. Attention has been given to flat premixed flames [45,46], as well as to the sampling of ions [47]. The perturbation of a flame depends on many factors, including the probe's characteristics. In particular, the quartz cone (inner angle 45°, wall thickness 1 mm) and its effect on the measured concentration of various species in a premixed flame of propene, oxygen, and argon have been studied [46]. The concentration profiles calculated using perturbed temperature profiles have been shown [46] to be affected by the probe differently: one group of concentration profiles was perturbed more than the other. Interestingly, these findings are consistent with the results obtained in the current work with a counterflow flame: the widening of the concentration profiles

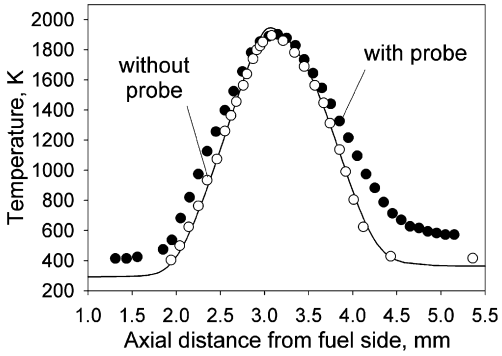

Fig. 8. Temperature profiles in the undoped counterflow flame. Symbols are thermocouple measurements on the flame's periphery ($r = 3.1$ mm) in front of the tip of the probe (at 0.2 mm from the tip) and without a probe. The curve is a calculated result along the axis.

of the lighter species H, OH, H_2O, and CO_2 not only because of upsets to the quasi-one-dimensional nature of the flame, but also due to significant perturbations by the probe.

To estimate how significant are the thermal perturbations, temperature profiles in the flame were measured with a thermocouple placed in front of the tip of the probe. In Fig. 8, temperature profile in the undoped flame, as measured by a thermocouple placed at 0.2 mm in front of the tip of the probe, which is situated at $r = 3.3$ mm from the axis, is presented. The calculated profile of temperature along the axis of the burner and the profile measured by the thermocouple without the probe are shown for comparison. One can see that the presence of the probe does not change the maximum flame temperature (within experimental error). However, it increases the temperature near the nozzles. The FWHM for the temperature profile measured with the probe present is observed to be ∼10% bigger than without the probe. This demonstrates that this probe slightly perturbs the counterflow flame.

Thus, it seems that measurements using MBMS can be predicted by a one-dimensional model, without taking into account perturbations by the probe, provided the species concerned has a high molecular weight (i.e., low diffusion coefficient). When concentration profiles of light species with high diffusivity are measured, a widening of the profiles in comparison with that predicted by the one-dimensional model is found. On the other hand, measured concentration profiles of reagents, which do have low molecular weights (CH_4, O_2), are consistent with the simulated ones. This is probably due to the structure of a real flame not being one-dimensional. This should be taken into account in comparing experimental and modeling (using the OPPDIF code) data.

The temperature in the flame reaches a maximum at approximately $l = 3.1$ mm (l is the distance from the fuel nozzle). One can distinguish two combustion zones in the flame (see Fig. 3): the first is the fuel-rich zone at $l < 3.1$ mm, and the second is the fuel-lean zone at $l > 3.1$ mm. An analysis of Fig. 7 leads to the following conclusions. The maximum concentration of $HOPO_2$ is in the fuel-lean flame zone, and the maximum concentration of HOPO is on the fuel-rich side. This accords with the measurements and modeling of premixed flames doped with TMP [27,40]: in a rich flame HOPO prevails over all the other P-species in the postflame zone, whereas in a lean flame the major P-bearing product in the postflame zone is $HOPO_2$. The peak concentrations of PO and PO_2 are near the maximum temperature. It is clear that the inhibition mechanism [28] predicts well the concentrations profiles of the measured P-bearing species.

5. Conclusions

The thermal structure of a counterflow flame has been examined with a microthermocouple; the concentration profiles of stable species such as CH_4, O_2, and CO_2 were measured by microprobe sampling and by MBMS. The microprobe did not disturb the flame. However, a sonic probe inserted into the flame transverse to the axis produced a significant disturbance of the flame. But no disturbance of the flame was observed when the tip of the sonic probe was located at the periphery of the burner. The concentration profiles of stable species measured by the microprobe and sonic probe at the periphery of the burner agreed with one another.

The concentration profiles of free hydrogen atoms, hydroxyl radicals, and the main phosphorus-bearing species (PO, PO_2, HOPO, $HOPO_2$) were measured by MBMS in the counterflow flame doped with TMP at the periphery of the burner and compared with profiles simulated using the OPPDIF Code and a combustion mechanism for organophosphorus compounds. Good agreement was obtained between measured and simulated concentration profiles for the final and intermediate products with high molecular weights (PO, PO_2, HOPO, $HOPO_2$). This fact validates the kinetic mechanism used for organophosphorus compounds [28]. The measured concentration profiles of final and intermediate species with low molecular weights (H_2O, CO_2, OH, H) were observed to be broader than the calculated ones; in fact, the lower the molecular weight, the wider is the profile. On the other hand, the measured concentration profiles of the reagents (CH_4, O_2, with low molecular weight) are consistent with the simulated ones. This is probably due to a real flame not being one-dimensional. The obtained results confirm the applicability of MBMS for measuring concentration profiles of species with

a relatively high molecular weight in opposed-jet flames.

Acknowledgments

This work was supported by INTAS under Grant 03-51-4724, the Russian Science Support Foundation, and the Siberian Branch of Russian Academy of Sciences under Grant for Young Scientists 76. The authors thank Professor A.N. Hayhurst for his assistance, fruitful discussion, and comments on our paper.

References

[1] S.C. Li, F.A. Williams, Proc. Combust. Inst. 28 (2000) 1031–1038.
[2] M.M.Y. Waly, F.A. Williams, Proc. Combust. Inst. 28 (2000) 2005–2012.
[3] R. Seiser, L. Truett, D. Trees, K. Seshadri, Proc. Combust. Inst. 27 (1998) 649–657.
[4] N.M. Marinov, W.J. Pitz, C.K. Westbrook, A.E. Lutz, A.M. Vincitore, S.M. Senkan, Proc. Combust. Inst. 27 (1998) 605–613.
[5] P. Berta, I.K. Puri, S.K. Aggarwal, Proc. Combust. Inst. 30 (2005) 447–453.
[6] A.N. Hayhirst, N.R. Telford, Proc. R. Soc. London Ser. A 322 (1971) 483–507.
[7] M.J. Height, K.E. Styan, E.M. Kennedy, B.Z. Dlugogorski, in: Proceedings of Halon Option Technical Working Conference, Center for Global Environmental Technologies, Albuquerque, NM, 1999, available at: http://www.bfrl.nist.gov/866/HOTWC/HOTWC2006/pubs/R9902752.pdf.
[8] M.F.M. Nogueira, E.M. Fisher, Combust. Flame 132 (2003) 352–363.
[9] E.W. Kaiser, T.J. Wallington, M.D. Hurley, J. Platz, H.J. Curran, W.J. Pitz, C.K. Westbrook, J. Phys. Chem. A 104 (2000) 8194–8206.
[10] R.T. Wainner, K.L. McNessby, R.G. Daniel, A.W. Miziolek, V.I. Babushok, in: Proceedings of Halon Option Technical Working Conference, Center for Global Environmental Technologies, Albuquerque, NM, 2000, p. 141.
[11] J.W. Hastie, D.W. Bonnell, Molecular Chemistry of Inhibited Combustion Systems, Final NBSIR 80-2169, PB81–170375, National Bureau of Standards, 1980.
[12] M.A. MacDonald, T.M. Jayaweera, E.M. Fisher, F.C. Gouldin, Combust. Flame 116 (1999) 166–176.
[13] R.R. Skaggs, R.G. Daniel, A.W. Miziolek, K.L. McNesby, in: Proceedings of the First Joint Meeting of the U.S. Sections of the Combustion Institute, Washington, DC, 1999, p. 575.
[14] V.I. Babushok, G.T. Linteris, W. Tsang, D. Reinelt, Combust. Flame 115 (1998) 551–560.
[15] A. Twarowski, Combust. Flame 94 (1993) 91–107.
[16] A. Twarowski, Combust. Flame 102 (1995) 55–63.
[17] A. Twarowski, Combust. Flame 105 (1996) 407–413.
[18] A.G. Shmakov, O.P. Korobeinichev, V.M. Shvartsberg, D.A. Knyazkov, T.A. Bolshova, I.V. Rybitskaya, Proc. Combust. Inst. 30 (2) (2004) 2342–2352.
[19] O.P. Korobeinichev, A.L. Mamaev, V.V. Sokolov, T.A. Bolshova, V.M. Shvartsberg, in: Proceedings of Halon Option Technical Working Conference, Center for Global Environmental Technologies, Albuquerque, NM, 2001, p. 173.
[20] O.P. Korobeinichev, V.M. Shvartsberg, A.A. Chernov, V.V. Mokrushin, Proc. Combust. Inst. 26 (1996) 1035–1042.
[21] O.P. Korobeinichev, A.A. Chernov, Combust. Flame 118 (1999) 718–726.
[22] J.H. Werner, T.A. Cool, Combust. Flame 117 (1999) 78.
[23] O.P. Korobeinichev, V.M. Shvartsberg, A.A. Chernov, Combust. Flame 118 (1999) 727–732.
[24] O.P. Korobeinichev, S.B. Ilyin, T.A. Bolshova, V.M. Shvartsberg, A.A. Chernov, Combust. Flame 121 (2000) 593.
[25] P.A. Glaude , H.J. Curran, W.J. Pitz, C.K. Westbrook, Proc. Combust. Inst. 28 (2001) 1749–1756.
[26] P.A. Glaude, C. Melius, W.J. Pitz, C.K. Westbrook, Proc. Combust. Inst. 29 (2002) 2469–2476.
[27] O.P. Korobeinichev, V.M. Shvartsberg, A.G. Shmakov, T.A. Bolshova, T.M. Jayaweera, C.F. Melius, W.J. Pitz, C.K. Westbrook, H. Curran, Proc. Combust. Inst. 30 (2) (2004) 2353–2360.
[28] T.M. Jayaweera, C.F. Melius, W.J. Pitz, C.K. Westbrook, O.P. Korobeinichev, V.M. Shvartsberg, A.G. Shmakov, T.A. Bolshova, H. Curran, Combust. Flame 140 (2005) 103–115.
[29] M.A. McDonald, F.C. Gouldin, E.M. Fisher, Combust. Flame 124 (4) (2001) 668–683.
[30] J.E. Siow, N.M. Laurendeau, Combust. Flame 136 (2004) 16–24.
[31] K. Seshadri, F.A. Williams, Int. J. Heat Mass Transfer 21 (1978) 251–253.
[32] O.P. Korobeinichev, A.G. Shmakov, V.M. Shvartsberg, D.A. Knyazkov, V.I. Makarov, K.P. Koutsenogii, Yu.N. Samsonov, E.E. Nifantev, I.Y. Kudryavtsev, E.I. Goryunov, V.P. Nikolin, V.I. Kaledin, in: Proceedings of Halon Option Technical Working Conference, Center for Global Environmental Technologies, Albuquerque, NM, 2003, available at: http://www.bfrl.nist.gov/866/HOTWC/HOTWC2003/pubs/R0301562.pdf.
[33] O.P. Korobeinichev, S.B. Il'in, V.M. Mokrushin, A.G. Shmakov, Combust. Sci. Technol. 116–117 (1996) 51–67.
[34] I.S. Grigorieva, E.Z. Meilihova (Eds.), Physical Values, Energoatomizdat, Moscow, 1991 [in Russian].
[35] W.E. Kaskan, Sixth Symposium (International) on Combustion, 1957, pp. 134–141.
[36] A.E. Lutz, R.J. Kee, J.F. Grcar, F.M. Rupley, Chemkin Collection, Unlimited Release, Sandia National Laboratories, Livermore, CA, 1997.
[37] R.J. Kee, F.M. Rupley, J.A. Miller, Chemkin-II: A Fortran Chemical Kinetics Package for the Analysis of Gas-Phase Chemical Kinetics, Report No. SAND89-8009B, Sandia National Laboratories, 1989.

[38] H.K. Chelliah, C.K. Law, T. Ueda, M.D. Smooke, F.A. Williams, Proc. Combust. Inst. 23 (1990) 503–510.
[39] G.P. Smith, D.M. Golden, M. Frenklach, N.W. Moriarty, B. Eiteneer, M. Goldenberg, C.T. Bowman, R.K. Hanson, S. Song, C. William, J. Gardiner, V.V. Lissianski, Z. Qin, GRI Mech 3.0, 1999, available at: http://www.me.berkeley.edu/gri_mech/.
[40] O.P. Korobeinichev, V.M. Shvartsberg, A.G. Shmakov, D.A. Knyazkov, I.V. Rybitskaya, Proc. Combust. Inst. 31 (2) (2007) 2741–2748.
[41] C. Melius, M.D. Allendorf, J. Phys. Chem. A 104 (2000) 2168–2177.
[42] N. Vora, J.E. Siow, N.M. Laurendeau, Combust. Flame 126 (2001) 1393–1401.
[43] C.E. Frouzakis, J. Lee, A.G. Tomboulides, K. Boulouchos, Proc. Combust. Inst. 27 (1998) 571–577.
[44] A.N. Hayhurst, D.B. Kittelson, N.R. Telford, Combust. Flame 28 (1977) 123–136.
[45] J.C. Biordi, C.P. Lazarra, J.F. Papp, Combust. Flame 23 (1) (1974) 73–82.
[46] A.T. Hartlieb, B. Atakan, K. Kohse-Hoinghaus, Combust. Flame 121 (2000) 610–624.
[47] A.N. Hayhurst, N.R. Telford, Combust. Flame 28 (1977) 67–80.